
Determining the Efficacy of a Silica and Bacterial Cellulose Composite Model System

A Senior Project
presented to
the Faculty of the Materials Engineering Department
California Polytechnic State University – San Luis Obispo

In partial fulfillment
of the requirements for the Degree
Bachelor of Science

Daisy Kamp & Hannah Martin
Under the Advisement of Dr. Trevor Harding & Dr. Leslie Hamachi
June 2022

Contents

1	Abstract	3
2	Motivations	4
2.1	The Environmental Impact of Leather	4
2.2	Sustainable Alternatives to Leather	5
3	Background	7
3.1	Bacterial Cellulose	7
3.2	Use of Silica Particles	10
3.3	Research Question	11
4	Methodology	12
3.1	Sample Synthesis	12
3.2	Scanning Electron Microscopy.....	14
3.3	Thermogravimetric Analysis	14
5	Results	15
4.1	SEM study of Surface Microstructural Characteristics	15
4.2	TGA Measurement of Composite Sample Silica Content	17
6	Discussion	20
7	Conclusions and Future Recommendations	23
8	References	24
9	Appendix	26

1 Abstract

Bacterial cellulose (BC) is a sustainable alternative to petroleum-based polymer films for synthetic leather applications. Synthesized by a symbiotic culture of bacteria and yeast, BC is a three-dimensional structure composed of cellulose microfibrils. However, pure BC lacks certain desirable properties such as high tensile strength. Previous studies have shown that loading BC with nanoparticles to form nanocomposites has improved BC's mechanical properties. However, this was not studied as a function of particle size. This study focuses on using silica/BC nanocomposites to model the impact that particle size and silica soaking concentrations have on the uptake efficiency of these particles into BC. Silica particles are incorporated into the BC hydrogel by diffusion, where 100 nm and 1300 nm silica particles at varying concentrations were tested. Scanning electron microscopy (SEM) was used to visually analyze the silica loading in the samples. The samples soaked with 1300 nm silica particles showed no visible particles on the film surface, while the samples soaked with 100 nm silica particles display a textured surface possibly attributable to silica particles on the surface of the BC. Thermogravimetric analysis (TGA) of the samples soaked with 1300 nm silica particles across all concentrations show no increase in silica weight percent, confirming our observations from SEM. However, the samples soaked with 100 nm silica particles showed an increase in inorganic residue of 2.23%, 4.11%, and 11.10% with increasing silica soaking concentration via TGA. Despite these findings, the data was not statistically significant to conclude successful increase in silica content with increasing soaking concentrations.

2 Motivations

By 2022, the leather goods market in the U.S. is estimated to reach US\$128.61 billion.¹ As a material, leather has a wide variety of uses and sources. Traditionally, leather is made from animal hides, primarily cattle hide, but the sources of leather have widened to include petroleum-based pseudo-leather also known as “pleather”, and other alternative sources. Leather finds use in a variety of applications: from more protective or structural applications in items such as shoes, furniture, or saddles, to more fashion-oriented applications in the form of clothing or personal accessories such as handbags. One reason that leather continues to be so popular as a textile is due to its association with quality products. This in part due to the tunable material properties that leather offers such as water resistance and thermal insulation, as well as variable malleability and high strength that depends on the thickness of the leather.² However, since 68% of all manufactured natural leather comes from the cattle industry,³ this brings up major environmental concerns about natural bovine leather due to the negative environmental impacts and ethics surrounding the bovine livestock industry.

2.1 The Environmental Impact of Leather

Escalating environmental concerns over climate change have brought the negative impacts of the leather industry into focus. On the surface, leather is easy to portray as a relatively environmentally harmless textile. Proponents of the leather industry argue that since leather is made from the byproduct of the bovine meat industry, it is a natural renewable resource, and natural leather is biodegradable at the end of its life.⁴ Upon closer examination however, leather is inherently tied to the major sustainability problems associated with the bovine industry, as well as the additional problems related to the environmental hazards of the leather tanning processes. The bovine livestock industry, where 99% of cow leather hides are sourced from, has severe environmental impacts such as greenhouse gas emissions, deforestation (particularly the Amazon rainforest in Brazil), as well as both water and land overuse.⁵ Even with all the negative impacts of the livestock industry excluded, the leather tanning process utilizes toxic chemicals such as chromium and formaldehyde that pollute surrounding waterways and pose extreme health risks to humans⁶ in countries without strict regulation. Additionally, the process of tanning turns biodegradable hides into non-biodegradable leather. Degradation studies have found that chromium tanned hides only reach 40% biodegradation after 2.5 months, while hides

undergoing more “natural” vegetable tanning reach 81% biodegradation in the same time period, which is still under the 90% specified for “full biodegradation” by the UNI EU standard.⁷ Synthetic leather is often proposed as an alternative, and the comparison of the environmental impact of the two materials can be seen in Figure 1, where the relative carbon cost of different textile leather goods is compared.

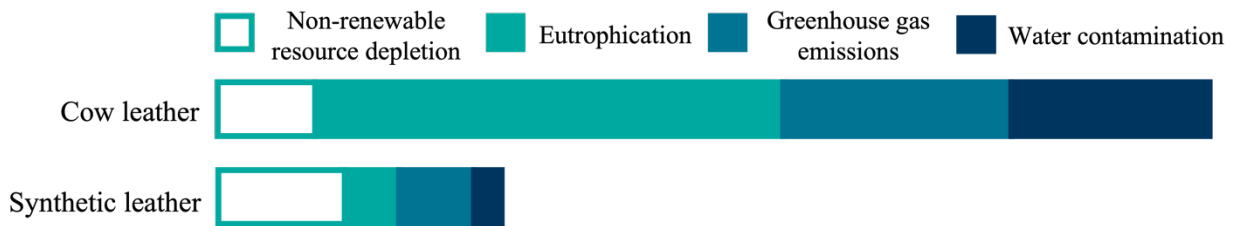


Figure 1. Comparison of the carbon cost of natural and synthetic leather goods.⁸

While artificial leather has a lower carbon emission impact, petroleum-based artificial leather has its own set of linked negative environmental hazards and qualities. The most common materials used for synthetic leather is a polyester base fabric with a top coating layer that is primarily polyvinyl chloride (PVC) or polyurethane (PU). While polyester-based leather has a comparatively lower environmental impact than natural leather, it is still an overall high impact process tied to the environmental problems of the petroleum industry and synthetic petrochemical-based polymers. Since artificial leather is made from polyester with a PVC or PU coating, it is non-degradable and once thrown away; and it will only break up into smaller and smaller microplastics that never completely degrade.⁹ Additionally, the multiple types of polymers bound together into the layered structure of artificial leather makes it difficult to recycle. Due to the downsides of both natural and synthetic leather, more innovative and sustainable alternatives must be studied to reduce the leather industry’s environmental impact while still meeting the rising global demand for leather.

2.2 Sustainable Alternatives to Leather

One sustainable solution for leather use is utilizing recycled natural leather or synthetic leather made from recycled polymers. Most recycled natural leather utilizes pre-consumer production scraps that are the bonded together to make a useable textile. Similarly, recycled synthetic leather is made from recycled polyurethane to minimize the fact that polyester-based materials are non-

biodegradable.⁵ While these solutions are certainly a step in the right direction, they cannot act as a long-term solution since each recycled fabric still utilizes the leather resulting from the environmentally harmful livestock industry or petrochemical industry.

Alternatively, there are a variety of more environmentally oriented leather substitutes being developed and sold in the textile market. These include plant-based alternative leathers such as cactus leather, or leather made from fruit waste such as discarded mangos or discarded pineapple leaves. However, the difficulty with these alternatives is that often polyurethane is used as a coating for the fabrics to increase durability. While this coating process makes these alternatives more desirable fabrics, it also negatively impacts their biodegradability and ties the product's success to the petrochemical industry.¹⁰ More recently, another leather alternative under development is bacterial cellulose. Bacterial cellulose is a sustainable biomaterial that can be grown using waste glucose sources such as sugarcane offcuts and bacteria. Due to its leather-like tactile feel, structure that offers tunable material properties, and the wide range of processing options for different textile results,¹¹ bacterial cellulose is a promising candidate as a leather alternative meriting further study.

3 Background

3.1 Bacterial Cellulose

Cellulose is the most abundant polymer on the planet, and can be found in plants, algae, fungi, and bacteria.¹² One form of cellulose comes from bacteria and is stronger than the cellulose found in plant cell walls. Bacterial cellulose (BC) is commonly grown with a *Gluconacetobacter xylinus* (*G. xylinus*) bacterial colony, where the cellulose is excreted from the bacteria when they are placed under extreme stress due to varying environmental conditions. Additionally, the bacteria need to be in a medium with a carbon source to grow the cellulose. This is usually supplied by glucose or fructose molecules, but can also come from other carbon rich food products.¹³ During excretion, the cellulose fibrils from the bacteria get tangled with each other, forming a hydrogel on the surface of the medium they are in. The hydroxyl groups off the main fibril structure also inhibit hydrogen bonding. This reinforces the secondary bonding within the fibrils and makes the BC strong. When grown in fermented tea, or kombucha, it is known as a Symbiotic Culture of Bacteria and Yeast (SCOBY). The structure of these fibrils are one-dimensional cellulose nanofibrils and have the chemical structure shown in Fig. 2.

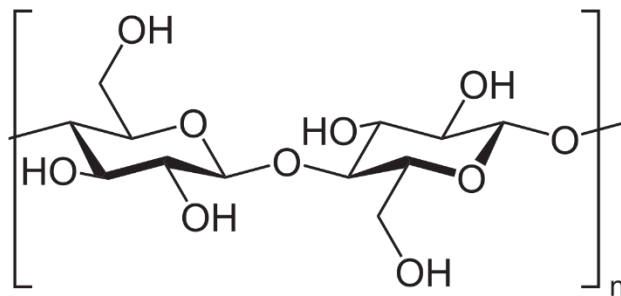


Figure 2. Cellulose repeating mer structure.

3.1.1 Positive and Negative Aspects of BC

Since a BC medium needs sources of carbon to form, this can be supplied by many natural and waste sources, decreasing the cost of production of BC. Waste products such as agro-industrial residues, rotten fruit, and wastewater from the nata de coco or sugarcane processing industries have all been proven sources that lead to successful synthesis of BC.¹³ Using these alternative sources utilizes materials that would otherwise be treated as waste and reduces the cost of the materials needed to produce BC. Additionally, the SCOBY growth process requires little external energy input for the bacterial cellulose to be grown since the bacteria facilitate the

growth process. However, the SCOBY growth process is traditionally done in batches, which is a noncontinuous processing method. SCOBYs must be grown one at a time after another, so at a small scale it would take a lot of time to obtain the materials needed to make a useable amount of textile material. This production reality is currently not favorable for large scale manufacturing of this product, but with continued research efforts has the potential to be translated to an industrial scale as semi-continuous and continuous batch processes are developed.¹⁴ Most of the current work being done in BC research is focused on the synthesis and improving mechanical and hydrophobic properties of it, and once solved will spur later efforts to mold the process to an industrial scale.

Another benefit to BC is that the cellulose fibril structure. During synthesis, BC takes on the woven fiber structure shown in Fig. 3, where each cellulose fiber is made up of many cellulose nanofibrils bound together, making it a relatively high strength material. This makes the material eligible for textile applications where it will be stretched under various stresses in different directions. Additionally, the hydrogen bonding in the fibril structure keeps the BC strong and prevents tearing of the material when dry. Together, the price of starting materials for BC and its high strength makes BC a desirable sustainable alternative to leather. However, the film is often not homogenous in thickness due to the uncontrolled nature of cellulose production using bacteria. This can affect the mechanical properties across the material, and leave some spots weaker than others, which are more likely to fracture than the stronger counterparts. Without strengthening the material in a different way, the weaker spots will be the driving force for fracture which is not desirable in a product.

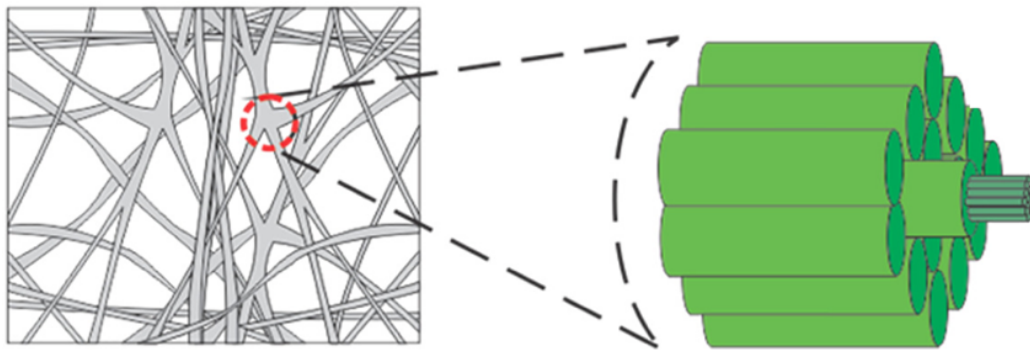


Figure 3. Nanoscale structure of cellulose fibrils in the bacterial cellulose fiber matrix.¹⁵

3.1.2 Possible Solutions to Improve BC Properties

To combat the inconsistencies in BC structure, researchers have previously investigated adding nanoparticles to improve the overall mechanical properties of the material. Iron oxide nanoparticles have been added to BC to improve the mechanical properties, and they also improve the electrical conductivity of BC.¹⁶ These particles have helped sustain the life of the BC with repeated electrical cycles and the associated thermal strain. However, these particles are not as effective on the mechanical properties other than thermal strain, so they are not the correct particles to be analyzing for leather purposes.

Some two-dimensional nanocomposites such as montmorillonite (MMT) clays have also been used in reinforcing BC.¹⁷ These nanoparticles have been proven to improve the mechanical and thermal properties of BC while staying biocompatible for biomedical applications. A downside to this nanoparticle is that it has a long and tedious processing procedure to synthesize the clay into nanoparticles. Additionally, MMT is difficult to completely disperse into BC and prevent agglomeration without extensive processing, making this BC composite difficult to effectively develop in research, and impractical for larger-scale industrial applications.

Another common nanoparticle used in nanocomposites is silica (SiO_2), which has been used in polymer matrices such as polyurethanes.¹⁸ The addition of these nanoparticles improved the modulus and tensile strength of the polymer at a 40% weight of silica. Since this nanoparticle has improved the properties of polymer matrices, researchers have attempted to use silica particles in BC matrices as well (Yano et al., 2008). The particles ended up ruining the crystallinity of the BC by interrupting the fibril structure in the cellulose. No further research has been done on using silica nanoparticles of smaller sizes, which is a possible route for research in silica BC composites. Using this nanoparticle is also more practical in research because of the associated ease of particle synthesis and lower material price. Additionally, as-synthesized silica particles are inorganic, which means they will be easy to distinguish from the organic molecule-based BC.

3.2 Use of Silica Particles

3.2.1 *Developing Silica Particles as a Model System*

One of the main advantages for studying silica particle and bacterial cellulose nanocomposite films is the opportunity to better understand the impact of particle size on uptake into BC, and how that may impact the material properties of BC. Silica particles are a relatively easy particle (in comparison to other nanoparticles mentioned above) to study since their size, porosity, crystallinity, and shape can be precisely manipulated, and because they have large-scale synthetic availability. Additionally, silica can be well-dispersed in polar solvents like water¹⁹ which would theoretically allow for high levels of homogenous diffusion into a BC SCOBY immersed in water during the production of a BC/silica composite. The relative ease of size modification and incorporation of silica particles into BC makes silica a desirable particle to use to investigate the impact of particle size on the success of particle incorporation and resulting bulk properties of BC, which has not been studied.

3.2.2 *Impact of Silica Particle Size*

Previous research groups have attempted to quantify the effect of the addition of silica particles to BC. In the research performed by Yano et al., silica nanoparticles of size 40-50nm were incorporated into BC. The group found that incorporating the silica nanoparticles into the crystalline BC matrix decreased the failure strength of the material. This was theorized to be due to the disruption of the inter-fibril hydrogen bonding as seen in Figure 4, where the silica nanoparticles disrupt the uniform crystalline structure of the bacterial cellulose.²⁰

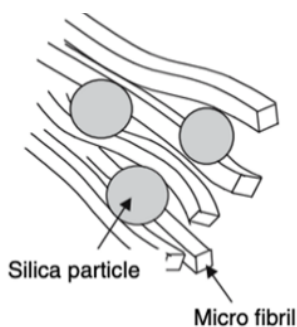


Figure 4. Disruption of the nanofibril structure of BC due to the addition of silica particles.²⁰

However, since the previous research only studied one size of nanoparticle, there is no data in the literature that gives insight to the correlation between silica particle size or concentration and the

resulting mechanical and physical properties of the resulting BC composite. This correlation could be important information when the silica/BC composite is considered as a model system. This could give insight into the impact of nanoparticles and microparticles of any type on the structure of bacterial cellulose and the efficacy of BC nanocomposites as a functional material.

3.3 Research Question

The goal of this research project is to investigate the difference in silica (SiO_2) nanoparticle versus microparticle diffusion into BC films synthesized by *Gluconacetobacter xylinus*. To evaluate this phenomenon, the following objectives must be investigated:

1. Confirm silica uptake for each particle size by analyzing percent residue using thermogravimetric analysis across multiple silica soaking concentrations and a control.
2. Visually determine if uptake of silica particles into the BC occurred using scanning electron microscopy.
3. Determine a model for the uptake of silica particles into BC as a function of silica weight percent and soaking concentration of each particle size.

Objective: Develop a model system that demonstrates the relationship between uptake efficiency of silica particles in BC films as a result of the particle size.

4 Methodology

4.1 Sample Synthesis

The kombucha SCOBY was synthesized in a sterile glass container inside a fume hood, following the process outlined in Figure 5. The culture medium was composed of the bacterial culture (*G. xylinus* and yeast) and a 1:1:10 ratio of apple cider vinegar, glucose, and steeped black tea. To prepare the culture medium, the water was boiled in a large beaker and then removed from heat before the black tea bag was added. The tea bag was left to steep for 15 minutes before removal. Next, sugar was added and stirred with a stir bar until fully dissolved. Once the solution had cooled (approximately 30 minutes), it was transferred to a sterile container and the apple cider vinegar and bacteria culture were added. A lid with porous but tightly woven cloth was placed on top of the container to control the air flow. The container was then placed on a heated mat at 80°C for four weeks to grow and was periodically checked to ensure no contamination had occurred. The fully grown SCOBY samples, also referred to as BC pellicles, ranged from 1.5-2cm in thickness across a pellicle. The pellicle was then cut up into smaller pieces to make the purification process easier (Figure 6a).

To ensure a neutral bacterial cellulose, the fully grown BC samples were put through a purification process to remove any remaining acetic acid. To do this, the BC pellicle pieces were submerged in 90°C NaOH at a 1.0M concentration for one hour and then rinsed with DI water. This step was repeated twice to ensure the samples were fully purified. Lastly, the BC pellicles were bleached in a 1.5% NaOCl solution for two hours at room temperature before being rinsed with DI water a final time (Figure 6b).

The silica nano- and microparticles were synthesized following a procedure by Nozawa et al. The 1300 nm sized particles were synthesized following the 0.5mL/min injection rate of TEOS and the 100 nm particles followed the procedure outlines in Nozawa's Table 1.²¹ The 100nm stock solution had a concentration of 2.267 mg/ml, while the 1300 nm stock solution had a concentration of 1.29 mg/ml. The 100 nm silica stock solution was modified to form three soaking solutions at concentrations 0.33x, 1x, 2.2x of the stock concentration. The 1300 nm silica stock solution was diluted to form three soaking solutions at concentration 0.1x, 0.33x and 0.75x of the stock concentration. The varying concentration values and dilution factors were

dependent on the colloidal stability of the silica particles. Each soaking solution for both particle sizes were then placed into individual jars with a purified BC sample. Finally, the purified BC samples were soaked for two weeks before being dried in an oven at 50°C for 20 hours (Figure 6c), resulting in samples 100-200 μm thick. Sample naming conventions and the associated particle sizes and concentrations are outlined in Table I. All samples studied for the purposes of this paper were sourced from the same batch of BC pellicles.

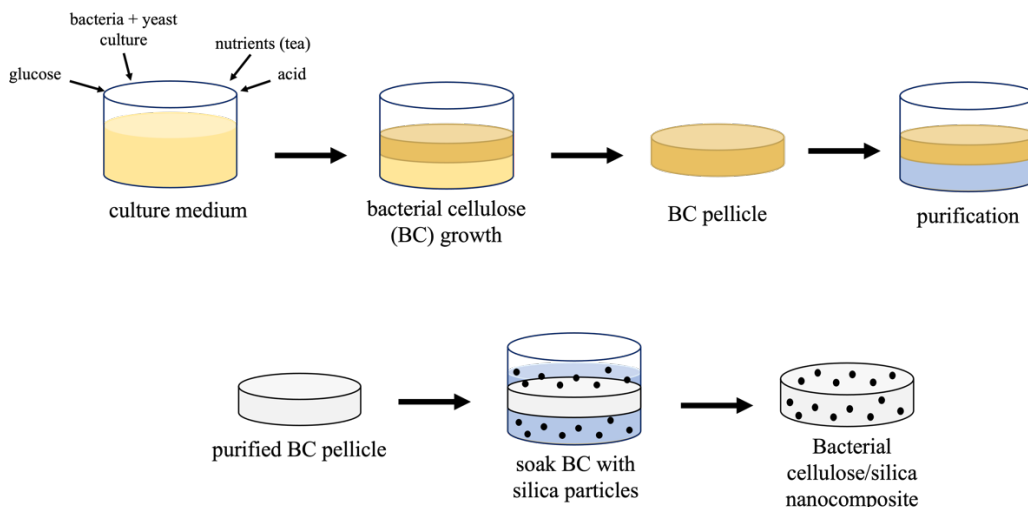


Figure 5. Preparation process of BC/silica nanocomposite samples.



Figure 6. BC samples throughout the preparation process: (a) unpurified but fully grown BC samples, (b) BC samples after purification, and (c) a soaked and dried BC/silica nanocomposite sample.

Table I. Compositions and Naming Conventions Used for BC/Silica Nanocomposite Samples.

Sample Designation	Silica Particle Size (nm)	Concentration Factor	Silica Solution Concentration (mg/mL)
BC_control	none	none	none
BC_100nm_0.33x	100	0.33x	0.748
BC_100nm_1x	100	1.0x	2.267
BC_100nm_2.2x	100	2.2x	4.987

BC_1300nm_0.1x	1300	0.1x	0.129
BC_1300nm_0.33x	1300	0.33x	0.426
BC_1300nm_0.75x	1300	0.75x	0.968

4.2 Scanning Electron Microscopy

Scanning electron microscopy (SEM) micrographs of the BC nanocomposite sample surfaces were taken on an FEI Quanta 200. The high-resolution imaging allowed for visual assessment of the sample surface structure and silica particle presence on the sample surface. To determine the structure of the silica particles as-synthesized, pure silica particles suspended in water were drop-cast onto individual silicon wafer squares with an average side length of 0.5 cm and left to dry for 24 hours. To image the surface of the BC samples, all samples were cut into a rectangular shape with average dimensions of 0.5cm x 1cm using a razor blade and were mounted horizontally. All samples were mounted on an aluminum pin stub mount using double-sided carbon tape to adhere the sample to the mount. After mounting, all samples were sputter coated with gold for thirty seconds before imaging to increase their interface conductivity and imaging resolution under high vacuum conditions. All samples were imaged under high vacuum, with an accelerating voltage of 30kV, a spot size of 3, and a scan speed of 94.25 seconds.

4.3 Thermogravimetric Analysis

Three replicates of each concentration and particle size were tested. Each sample was cut with a hole puncher to fit into the 90 μ L alumina pan and weighed to approximately 5mg. The sample was ramped up to 550°C at 10°C/min and held at an isothermal for 5 minutes before cooling to room temperature. The weight change was analyzed to obtain the percent residue. The inorganic matter left in the residue was assumed to be the silica content of the BC. This value was compared to the control residue to calculate the inorganic residue % silica that had diffused into the BC.

5 Results

5.1 SEM Study of Surface Microstructural Characteristics

Visual assessment of pure silica particles was performed via SEM at 20,000x for the 1300 nm (Figure 7a) and 100 nm (Figure 7b) particle sizes. Both samples show a variety of particle shapes and sizes, which is consistent with the observed size distributions for the as-synthesized 100 nm and 1300 nm diameter samples. The micrographs seem to show some agglomeration of particles, particularly for the 100nm sample. This agglomeration is possibly an artifact of the drying caused by the drop-casting method used to produce the samples or could be the standard shape of the as-synthesized particles.

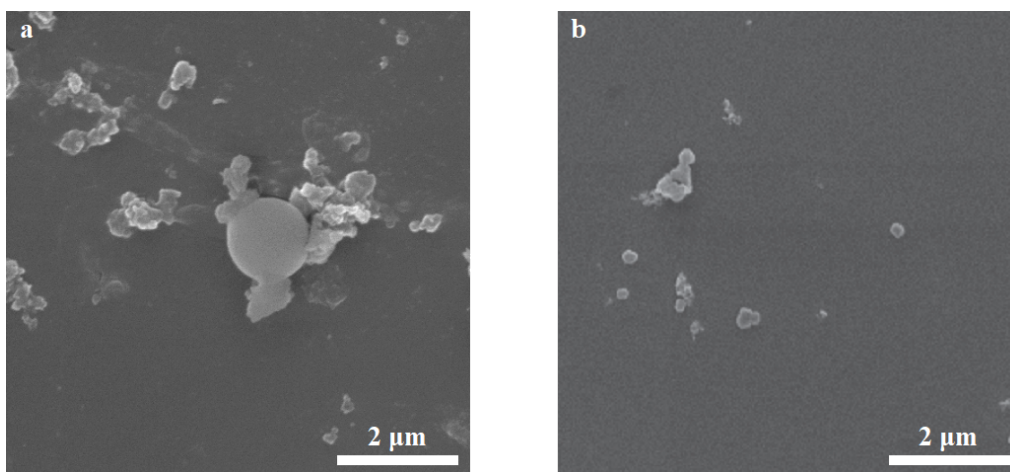


Figure 7. Representative SEM micrographs of drop-cast **(a)** 1300nm silica particles, and **(b)** 100nm silica particles.

Surface characterization of a pure bacterial cellulose sample from the same batch as the composite samples was performed at 15,000x (Figure 8). The surface morphology has the characteristic structure of woven cellulose fibers layered together during the growth of the SCOBY and preserved during the sample preparation process. While there are many individual fibers, the surface appears to be relatively flat and uniformly textured.

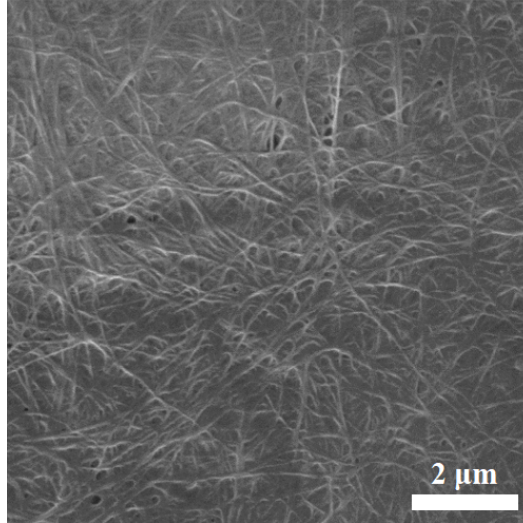


Figure 8. Representative SEM micrograph of a pure bacterial cellulose sample (BC_control) sourced from the same batch as the nanocomposite samples studied.

Surface characterization of the 1300 nm silica/BC composite sample (Figure 9) and 100 nm silica/BC composite sample (Figure 10) was performed at both 100x and 15,000x. In the macro-scale perspective of the 1300 nm silica/BC nanocomposite sample in Fig. 9a, there seems to be two visually different regions. Fig. 9b is a closer examination of the area in the blue square in Fig. 9a, while Fig. 9c is a closer examination yellow square in Fig. 9a. Fig. 9b is relatively consistent with the surface morphology of the pure bacterial cellulose sample, with a small amount of 1300 nm silica particles present on the surface. However, Fig. 9c shows a very different surface morphology, which appears to have cellulose fibers lifted off the surface of the sample and entangled with a higher amount of silica particles.

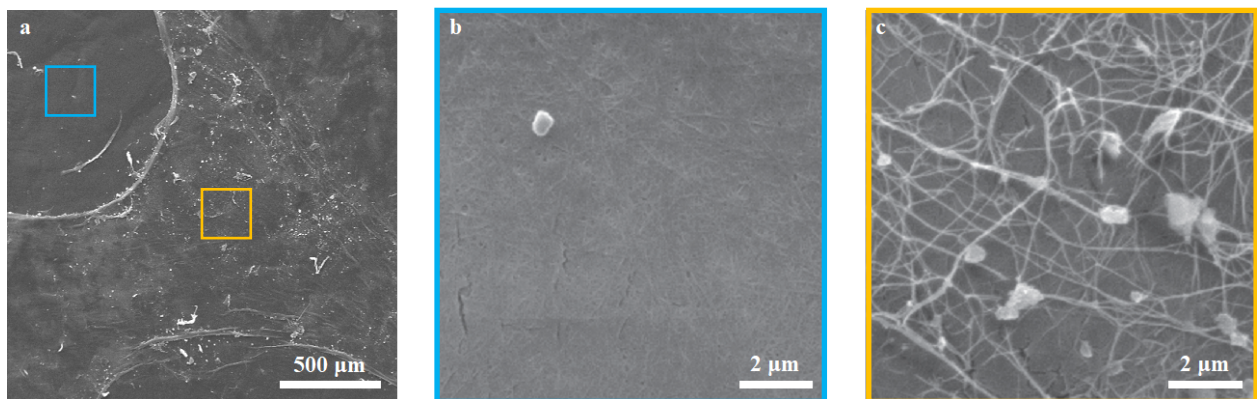


Figure 9. Representative micrographs of a BC_1300nm_0.33x sample at (a) 100x, (b) magnified to 15,000x in the upper left corner of micrograph 9a, and (c) magnified to 15,000x in the middle of micrograph 9a.

Similarly, the macro-scale perspective of the 100 nm silica/BC nanocomposite sample in Fig. 10a again seems to have two visually different regions. Fig. 10b is a closer examination of the area in the blue square in Fig. 10a, while Fig. 10c is a closer examination of the yellow square in Fig. 10a. Again, Fig. 10b is relatively consistent with the surface morphology of the pure bacterial cellulose sample, with a slightly increased amount of 100 nm silica particles seemingly present on or right below the surface. However, Fig. 10c shows the other surface morphology, which again appears to have cellulose fibers lifted off the surface of the sample and entangled with a higher amount of silica particles.

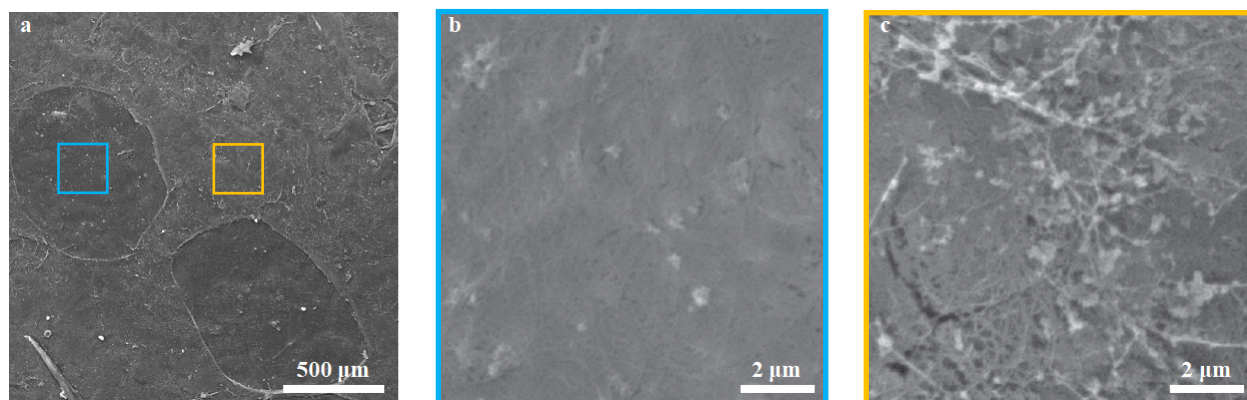


Figure 10. Representative micrographs of a BC_100nm_0.33x sample at (a) 100x, (b) focused to 15,000x on the left circle in micrograph 10a, and (c) magnified to 15,000x in the upper right corner of micrograph 10a.

5.2 TGA Measurement of Composite Sample Silica Content

The control BC sample showed an average percent residue of 29.64 (standard deviation of +/- 2.8), and the 1300 nm and 100 nm samples were directly compared to this value to determine silica uptake. The 1300 nm comparison shown in Figure 11 compares the average of each concentration with the control. The BC_1300nm_0.33x sample has the lowest percent residue, followed by the BC_1300nm_0.1x and BC_1300nm_0.75x. The control has the same residue left over as the BC_1300nm_0.75x, and the other samples were recorded to be below the control. All resulting 1300 nm particle composites did not observe an uptake of silica from a quantitative perspective.

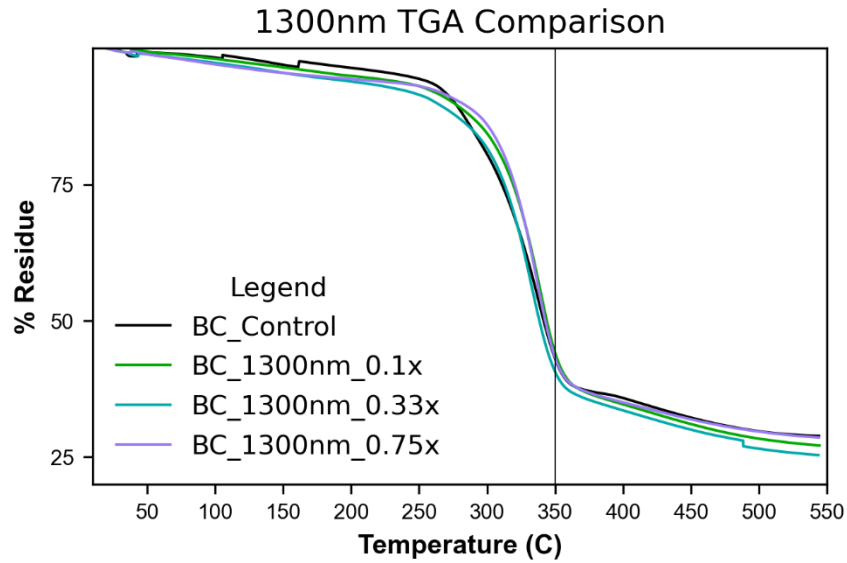


Figure 11. Representative TGA graph of the 1300 nm composites with the theoretical degradation of BC at 350°C

The 100 nm composite samples showed an increase in percent residue with increasing soaking concentration (Figure 12). The BC_100nm_0.33x sample had the lowest soaking concentration and had an increase in 2.23% residue from the control. The 1.0x and 2.2x concentration increased 4.11% and 11.10% respectively with respect to the control. The average percent residue values for all concentrations can be found in Appendix I.

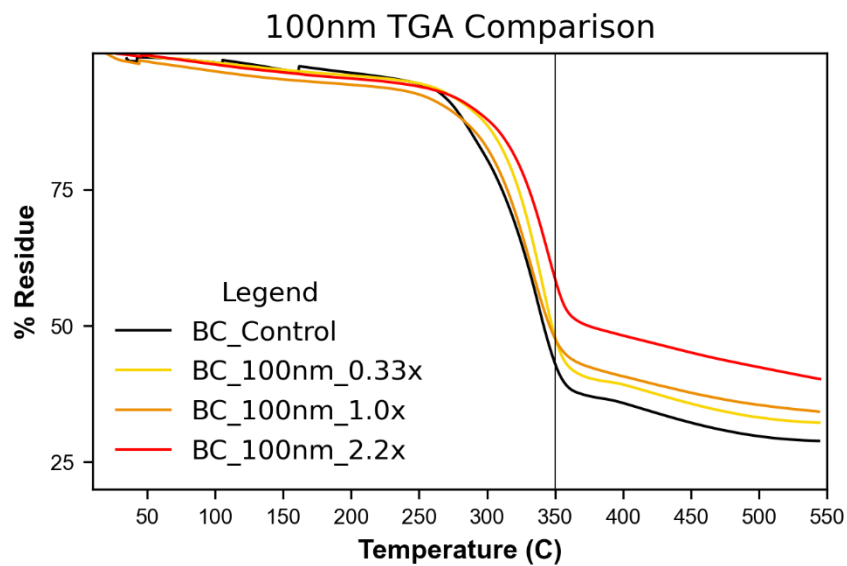


Figure 12. Representative TGA graph of the 100 nm composites with the theoretical degradation of BC at 350°C

The resulting percent residue for all samples is summarized in Figure 13, where the variability within samples can be seen in the error bars. The 1300 nm samples have low variability among the concentrations and their average percent residue change is minimal. The major overlap between soaking concentrations also implies no significant difference between processing methods. Analysis of variance (ANOVA) tests were run to prove statistical insignificance and can be found in Appendix II for the 1300 nm samples. The 100 nm samples show a mean increase in percent residue, but as the soaking concentration increases, the variability increases. With increasing variability, there is no significant difference in the soaking concentrations when comparing percent residue. The ANOVA test for the 100 nm samples can be found in Appendix III.

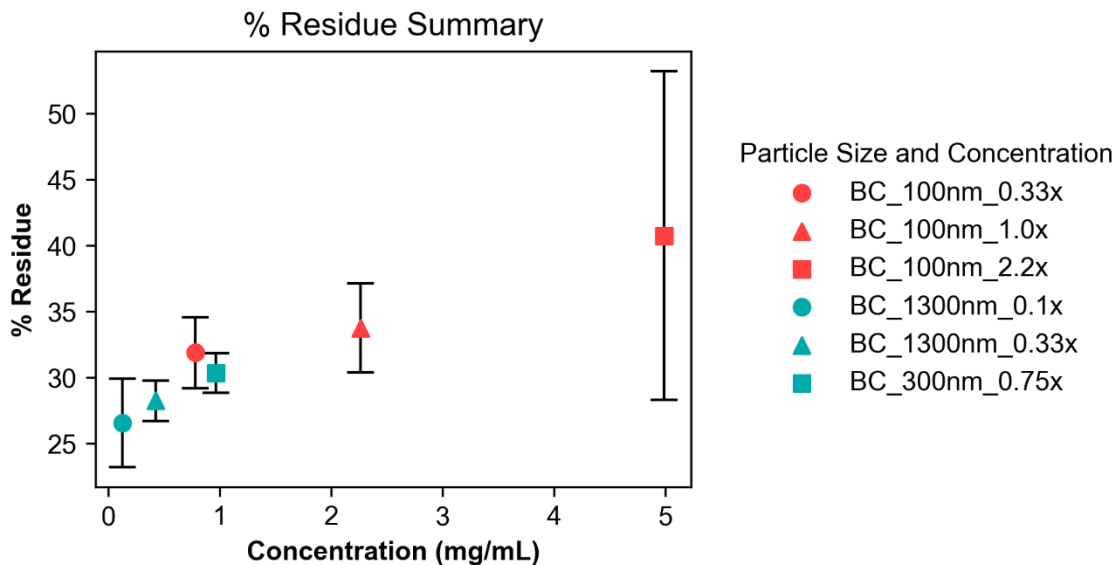


Figure 13. Summary TGA residue comparison across all samples expressed in average values with corresponding data variability.

6 Discussion

The combined results of the visual and thermal analysis of the different BC/silica composite samples seems to be consistent with the idea that as particle size decreases, particle uptake increases. Comparison of the SEM micrographs between the BC_100_0.33x and the BC_1300nm_0.33x samples seems to show an increased interaction between the surface of the BC and the silica particles as particle size decreases. Figure 8 of the BC_control sample seems to show good interfacial adhesion between the bacterial cellulose fibers, which can be similarly found in Fig. 9b and Fig. 10b which show similar surface structure. However, Fig. 9c and Fig. 10c seem to show decreased interfacial adhesion between the cellulose fibers, which has caused more silica particles to become entangled on the surface of the samples rather than diffusing in as expected.

In a paper published by Ashori et al. in 2012, the FE-SEM micrographs of their BC/silica composite samples showed similar surface structure to Fig. 9b and Fig. 10b, particularly with the BC_100nm_0.33x sample where the silica particles appear to be sitting in between cellulose fibers on the surface of the sample. The samples studied by Ashori et al. were synthesized using a very similar synthesis method, with the only significant differences being found in the fact that the silica particles were around 10-20nm in size, and the BC/silica nanocomposite samples were hot pressed (120°C at 2 MPa for 8-12 minutes) rather than oven dried at the end of their preparation.²² Due to the silica particles being a full size smaller in magnitude than the particles studied here, the increased presence and interaction between the BC surface and silica nanoparticles is consistent with the idea that decreasing particle size increases BC/silica interaction and success of particle diffusion into the BC during processing. One possible explanation for the lack of lifted cellulose fiber structures in the Ashori et al. paper that were observed in this study (Fig. 9c and Fig. 10c) could be attributed to the hot pressing processing step used that would likely have compressed any lifted surface structures.

Similarly, the paper by Yano et al. published in 2008 shows surface structures that were observed using atomic force microscopy (AFM) that are comparable to the structures observed here and in the Ashori et al. paper. The samples studied by Yano et. al. were synthesized by a similar process used here, but again soaked the BC pellicles in a 20nm silica nanoparticle

solution before utilizing the same hot pressing method, alongside oven drying the samples for 1-2 days at 100°C after the hot pressing was completed. Similar conclusions can be reached about decreased particle size increasing particle diffusion and presence on the sample surface, along with the hot pressing removing any lifted cellulose fiber surface structures. Additionally, it is important to note that Yano et al. hypothesized that since BC nanofibril and fiber formation is completed before silica is introduced into the system, the silica particles diffuse into the interfacial spaces between the cellulose fibers.²⁰ This mechanism of silica incorporation via diffusion would then result in much less silica particle incorporation into the BC matrix, making the successful incorporation of silica particles via diffusion particularly dependent on particle size. This explanation would help support the evidence found that the larger 1300 nm silica particles had little to no interaction with the flat surface of the BC sample since the size of these particles is much larger than the interfacial spaces between cellulose fibers. The 100 nm silica particles should then more easily diffuse into the BC fiber structure due to their smaller size, which can be seen in the micrographs collected here. Finally, the 10-20 nm particles used in the Ashori et al. and Yano et al. papers would have the most incorporation via diffusion, which is corroborated by the data given in those papers.

After quantitative analysis of silica uptake among the BC/silica nanocomposites, the 1300 nm data implies no silica uptake, while the smaller 100 nm particles have an increase in mean % residue but also a corresponding increase in variability. The lack of diffusion for the 1300 nm particles can likely be attributed to their large size in comparison to the interfacial spaces of the BC fibers. The 100 nm silica uptake mirrors data from Yano et al., where there is an increase up to 10% silica content with increasing silica soaking concentration. However, Yano et al. synthesized their nanocomposites with silica particles close to 20 nm, which is significantly smaller than our silica nanoparticle size. The findings of Yano et al. corroborates the trends found in the 100 nm silica composite samples but further testing with smaller particles sizes should be done, in order to draw more concrete conclusions. Similar conclusions were also made in a paper by Maeda et al., where there was an increase in silica content by 4% when doubling the soaking concentration of the silica.²³ Although Maeda et al. uses a silanol solution rather than pure silica for particle uptake, it shows a relationship with soaking concentration that was observed in the TGA data in this experiment.

The large amount of variability in our samples is likely due to the heterogeneity of the BC sheets. After the drying process, there were varying thicknesses across the sample which may have affected the quantitative analysis of the BC. Since the thickness of the sample varied, during the silica soaking stage there may have been patches of excess voids for silica to diffuse into, where other areas had an insufficient amount of interfibrillar spaces for silica diffusion. Additionally, each BC pellicle varied in thickness even within a single sample, which could have had an impact on the uptake of silica into different regions, where thicker regions would theoretically have more space for silica particles to diffuse into. This would result in inconsistent TGA data, which can leave results inconclusive.

7 Conclusions and Future Recommendations

After further visual and quantitative analysis of the BC/silica composites, the results are consistent with the idea that there is an inverse relationship between silica particle size and particle uptake. As the particle size decreases, there was an observed increase in % residue from TGA and more particles were observed on the surface of the BC. However, the resolution of the micrographs and statistical analysis of the data proves no statistical significance in the difference among soaking concentrations. For more robust and conclusive data, additional TGA experiments should be run for each soaking concentration to potentially determine a relationship between the soaking concentration and silica uptake.

The silica interactions with the BC showed two distinguishable morphologies on the surface of the BC, one consistent with the control and one with the fibers being entangled with the silica. Future research should explore the chemical interactions between silica and the surface of the BC to investigate the morphology differences. Additionally, further research should be done that focuses on the effect that different BC sample processing methods have on sample morphology. The use of hot pressing versus oven drying may influence the final structure and material properties of the BC.

For future experiments, data should be taken among multiple batches of BC. This experiment was run on one BC pellicle, and characterization across multiple pellicles would confirm if our synthesis process is replicable. Furthermore, the current BC synthesis process results in BC films of varying thicknesses, which could cause inconsistencies in data even within a singular BC pellicle. More replicate testing across the same BC pellicle and multiple different BC pellicles would increase the robustness of the data, minimizing outlying data points that would have much larger influence in smaller data sets.

8 References

- (1) *Global Leather Goods Market Size, Demand Forecasts, Industry Trends & Updates (2018-2025)*. businesswire.
<https://www.businesswire.com/news/home/20181005005348/en/Global-Leather-Goods-Market-Size-Demand-Forecasts-Industry-Trends-Updates-2018-2025---ResearchAndMarkets.com> (accessed 2021-12-02).
- (2) *Leather Naturally - Why Use Leather? Characteristics & Properties of Leather | Leather Naturally*. <https://www.leathernaturally.org/Education/Fact-Sheets/Benefits/Why-use-leather-The-characteristic-and-properties> (accessed 2021-12-05).
- (3) 2020 Preferred Fiber and Materials Market Report (PFMR) Released! - Textile Exchange.
- (4) *Where Does Leather Come From?*. MAHI Leather.
<https://mahileather.com/blogs/news/where-does-leather-come-from> (accessed 2021-12-06).
- (5) *Fibre Briefing: Leather*. Common Objective.
<http://www.commonobjective.co/article/fibre-briefing-leather> (accessed 2021-12-06).
- (6) *Leather*. Collective Fashion Justice. <https://www.collectivefashionjustice.org/leather> (accessed 2021-12-06).
- (7) Italian Leather Research Institute. *SSIP is attempting to measure the biodegradability*. Tannery Magazine. <http://https%3A%2F%2Ftannerymagazine.com%2FSSIP-biodegradability%2F> (accessed 2021-12-06).
- (8) *Higg Index*. <https://portal.higg.org/user-registration/login> (accessed 2022-06-06).
- (9) *Fibre Briefing: Polyester*. Common Objective.
<http://www.commonobjective.co/article/fibre-briefing-polyester> (accessed 2021-12-06).
- (10) *Leather alternatives*. Collective Fashion Justice.
<https://www.collectivefashionjustice.org/leather-alternatives> (accessed 2021-12-06).
- (11) Rathinamoorthy, R.; Kiruba, T. Bacterial Cellulose—A Sustainable Alternative Material for Footwear and Leather Products. In *Leather and Footwear Sustainability: Manufacturing, Supply Chain, and Product Level Issues*; Muthu, S. S., Ed.; Textile Science and Clothing Technology; Springer: Singapore, 2020; pp 91–121.
https://doi.org/10.1007/978-981-15-6296-9_5.
- (12) Muthu, S. S.; Rathinamoorthy, R. *Bacterial Cellulose: Sustainable Material for Textiles; Sustainable Textiles: Production, Processing, Manufacturing & Chemistry*; Springer Singapore: Singapore, 2021. <https://doi.org/10.1007/978-981-15-9581-3>.
- (13) Revin, V.; Liyaskina, E.; Nazarkina, M.; Bogatyreva, A.; Shchankin, M. Cost-Effective Production of Bacterial Cellulose Using Acidic Food Industry by-Products. *Brazilian Journal of Microbiology* **2018**, *49*, 151–159. <https://doi.org/10.1016/j.bjm.2017.12.012>.
- (14) Gama, F.; Gatenholm, P.; Klemm, D. *Bacterial Nanocellulose: A Sophisticated Multifunctional Material*; 2016; p 274.

- (15) Torres, F. G.; Arroyo, J. J.; Troncoso, O. P. Bacterial Cellulose Nanocomposites: An All-Nano Type of Material. *Materials Science and Engineering: C* **2019**, *98*, 1277–1293. <https://doi.org/10.1016/j.msec.2019.01.064>.
- (16) Huang, Y.; Lin, Z.; Zheng, M.; Wang, T.; Yang, J.; Yuan, F.; Lu, X.; Liu, L.; Sun, D. Amorphous Fe₂O₃ Nanoshells Coated on Carbonized Bacterial Cellulose Nanofibers as a Flexible Anode for High-Performance Lithium Ion Batteries. *Journal of Power Sources* **2016**, *307*, 649–656. <https://doi.org/10.1016/j.jpowsour.2016.01.026>.
- (17) Ul-Islam, M.; Khan, T.; Park, J. K. Nanoreinforced Bacterial Cellulose–Montmorillonite Composites for Biomedical Applications. *Carbohydrate Polymers* **2012**, *89* (4), 1189–1197. <https://doi.org/10.1016/j.carbpol.2012.03.093>.
- (18) Malay, O.; Oguz, O.; Kosak, C.; Yilgor, E.; Yilgor, I.; Menciloglu, Y. Z. Polyurethaneurea–Silica Nanocomposites: Preparation and Investigation of the Structure–Property Behavior. *Polymer* **2013**, *54* (20), 5310–5320. <https://doi.org/10.1016/j.polymer.2013.07.043>.
- (19) *Properties and Applications of Silica Nanoparticles - CD Bioparticles*. https://www.cd-bioparticles.com/t/Properties-and-Applications-of-Silica-Nanoparticles_57.html (accessed 2021-12-06).
- (20) Yano, S.; Maeda, H.; Nakajima, M.; Hagiwara, T.; Sawaguchi, T. Preparation and Mechanical Properties of Bacterial Cellulose Nanocomposites Loaded with Silica Nanoparticles. *Cellulose* **2008**, *15* (1), 111–120. <https://doi.org/10.1007/s10570-007-9152-x>.
- (21) Nozawa, K.; Gailhanou, H.; Raison, L.; Panizza, P.; Ushiki, H.; Sellier, E.; Delville, J. P.; Delville, M. H. Smart Control of Monodisperse Stöber Silica Particles: Effect of Reactant Addition Rate on Growth Process. *Langmuir* **2005**, *21* (4), 1516–1523. <https://doi.org/10.1021/la048569r>.
- (22) Ashori, A.; Sheykhnazari, S.; Tabarsa, T.; Shakeri, A.; Golalipour, M. Bacterial Cellulose/Silica Nanocomposites: Preparation and Characterization. *Carbohydrate Polymers* **2012**, *90* (1), 413–418. <https://doi.org/10.1016/j.carbpol.2012.05.060>.

9 Appendix

9.1 Appendix I: Average % residue concentrations (TGA) for all samples

Sample Name	Particle Size	Dilution	Conc (mg/mL)	% Residue
BC_100nm_0.33x_1	100	0.33x	0.74811	33.399
BC_100nm_0.33x_2	100	0.33x	0.74811	34.133
BC_100nm_0.33x_3	100	0.33x	0.74811	28.086
BC_100nm_1.0x_1	100	1x	2.267	37.12
BC_100nm_1.0x_2	100	1.0x	2.267	29.131
BC_100nm_1.0x_3	100	1x	2.267	34.99
BC_100nm_2.2x_1	100	2.2x	4.9874	57.53
BC_100nm_2.2x_2	100	2.2x	4.9874	37.0
BC_100nm_2.2x_3	100	2.2x	4.9874	27.68
BC_1300nm_0.1x_1	1300	0.1x	0.129	31.209
BC_1300nm_0.1x_2	1300	0.1x	0.129	24.835
BC_1300nm_0.1x_3	1300	0.1x	0.129	23.568
BC_1300nm_0.33x_1	1300	0.33x	0.4257	29.801
BC_1300nm_0.33x_2	1300	0.33x	0.4257	28.698
BC_1300nm_0.33x_3	1300	0.33x	0.4257	26.159
BC_1300nm_0.75x_1	1300	0.75x	0.9675	32.115
BC_1300nm_0.75x_2	1300	0.75x	0.9675	30.485
BC_1300nm_0.75x_3	1300	0.75x	0.9675	28.422

9.2 Appendix II: ANOVA test values for 1300 nm silica composite samples

Source of Variation	SS	df	MS	F	P-value	F crit
Between Groups	16.76388	3	5.58796	0.8784	0.523385	6.591382
Within Groups	25.44608	4	6.361521			
Total	42.20996	7				

9.3 Appendix III: ANOVA test values for 100 nm silica composite samples

Source of Variation	SS	df	MS	F	P-value	F crit
Between Groups	130.9602	2	65.4801	0.752	0.511182	5.143253
Within Groups	522.4476	6	87.0746			
Total	653.4078	8				